Original article

Nuclear Medicine Communications

Area at risk can be assessed by iodine-123-meta-iodobenzylguanidine single-photon emission computed tomography after myocardial infarction: a prospective study

Christophe Hedon[a,*], Fabien Huet[a,d,*], Fayçal Ben Bouallegue[b], Hélène Vernhet[c], Jean-Christophe Macia[a], Thien-Tri Cung[a], Florence Leclercq[a], Stéphane Cade[a], Frédéric Cransac[a], Benoit Lattuca[a], D'Arcy Vandenberghe[a], Aurélie Bourdon[b], Meriem Benkiran[b], Fabien Vauchot[b], Richard Gervasoni[a], Emmanuel D'estanque[b], Denis Mariano-Goulart[b,d] and François Roubille[a,d]

Background **Myocardial salvage is an important surrogate endpoint to estimate the impact of treatments in patients with ST-segment elevation myocardial infarction (STEMI).**

Aim **The aim of this study was to evaluate the correlation between cardiac sympathetic denervation area assessed by single-photon emission computed tomography (SPECT) using iodine-123-meta-iodobenzylguanidine (^{123}I-MIBG) and myocardial area at risk (AAR) assessed by cardiac magnetic resonance (CMR) (gold standard).**

Patients and methods **A total of 35 postprimary reperfusion STEMI patients were enrolled prospectively to undergo SPECT using ^{123}I-MIBG (evaluates cardiac sympathetic denervation) and thallium-201 (evaluates myocardial necrosis), and to undergo CMR imaging using T2-weighted spin-echo turbo inversion recovery for AAR and postgadolinium T1-weighted phase sensitive inversion recovery for scar assessment.**

Results **^{123}I-MIBG imaging showed a wider denervated area (51.1 ± 16.0% of left ventricular area) in comparison with the necrosis area on thallium-201 imaging (16.1 ± 14.4% of left ventricular area, $P < 0.0001$). CMR and SPECT provided similar evaluation of the transmural necrosis ($P = 0.10$) with a good correlation ($R = 0.86$, $P < 0.0001$). AAR on CMR was not different compared with the denervated area ($P = 0.23$) and was adequately correlated ($R = 0.56$, $P = 0.0002$). Myocardial salvage evaluated by SPECT imaging (mismatch denervated but viable myocardium) was significantly higher than by CMR ($P = 0.02$).**

Conclusion **In patients with STEMI, ^{123}I-MIBG SPECT, assessing cardiac sympathetic denervation may precisely evaluate the AAR, providing an alternative to CMR for AAR assessment.** ***Nucl Med Commun*** **00:000–000**

Nuclear Medicine Communications 2017, **00**:000–000

Keywords: area at risk, cardiac magnetic resonance, ^{123}I-MIBG SPECT, myocardial infarction, sympathetic denervation

Departments of [a]Cardiology, [b]Nuclear Medicine, [c]Cardiovascular Imaging, Montpellier University Hospital and [d]PhyMedExp, University of Montpellier, INSERM U1046, CNRS UMR 9214, Montpellier, France

Correspondence to François Roubille, MD, PhD, Department of Cardiology, Hôpital Arnaud de Villeneuve, CHU de Montpellier, UFR de Médecine, Université Montpellier 1, 371, avenue du Doyen Gaston Giraud, 34295 Montpellier cedex 05, France
E-mail: francois.roubille@gmail.com

*Christophe Hedon and Fabien Huet contributed equally to the writing of this article.

Received 27 June 2017 **Revised** 12 October 2017 **Accepted** 24 October 2017

Introduction

The occlusion of the culprit coronary artery leads to ischemia of the depending myocardium, defining the area at risk (AAR) [1]. Maintenance of myocardial viability is the goal of reperfusion therapy during acute ST-segment elevation myocardial infarction (STEMI) [2]. Myocardial salvage is defined as the amount of myocardium that is jeopardized by a coronary occlusion but spared from infarction and can be used to compare different cardioprotective approaches [3]. Noninvasive imaging techniques that can differentiate regions of reversible and irreversible myocardial injury *in vivo* are needed. Single-photon emission computed tomography (SPECT) for MRI with technetium-based radiotracers has been used widely to assess myocardial AAR [4]. Cardiac magnetic resonance (CMR) has been proposed for the assessment of myocardial edema on T2-weight protocols, providing an accurate estimation of the AAR, and is nowadays considered the noninvasive reference standard technique [3].

Supplemental Digital Content is available for this article. Direct URL citations appear in the printed text and are provided in the HTML and PDF versions of this article on the journal's website, *www.nuclearmedicinecomm.com*.

0143-3636 Copyright © 2017 Wolters Kluwer Health, Inc. All rights reserved.

DOI: 10.1097/MNM.0000000000000782

Interestingly, CMR can define both myocardial infarction and myocardial salvage at once [5].

Some basic studies have established the disruption of cardiac sympathetic nerve fibers (i.e. cardiac sympathetic denervation) following transmural myocardial infarction within viable myocardium in the distal segments of the site of intervention [6,7]. Alterations in myocardial sympathetic activity can be assessed by SPECT imaging using iodine-123-meta-iodobenzylguanidine (^{123}I-MIBG) [8,9]. Myocardial sympathetic nervous system is involved in maintaining cardiovascular homeostasis [10]. This is well established in patients with heart failure (HF) and chronic ischemic cardiomyopathy: cardiac denervation has been shown to be a predictor of worse outcome, increased risk of arrhythmia, and overall mortality [11,12].

By contrast, its significance remains unclear in patients with acute STEMI. In studies with small numbers of patients, it was suggested that sympathetic neuronal damage measured by ^{123}I-MIBG SPECT could estimate the AAR because of the high sensitivity of neuronal structures toward ischemia compared with myocardial cells [13,14].

Considering all these findings, we believe that ^{123}I-MIBG SPECT imaging could provide information on AAR soon after reperfusion. This approach could provide a new reliable tool for assessing this parameter critical for the individual assessment of cardioprotective strategies.

The aim of this study was to evaluate the correlation between cardiac sympathetic denervation assessed by ^{123}I-MIBG SPECT and the AAR assessed by CMR following reperfused STEMI.

Patients and methods

Study population and design

Consecutive patients were included between January 2014 and December 2014 in the Intensive Cardiology Care Unit of Montpellier University Hospital (France) after their admission for acute STEMI. Informed consent was obtained from each patient and the study protocol conformed to the ethical guidelines of the 1975 Declaration of Helsinki as reflected in a-priori approval by the institution's human research committee. They all had a primary percutaneous coronary intervention within the 24 h after the onset of symptoms.

All patients performed SPECT cardiac imaging assessment by dual isotope thallium-201 (^{201}Tl) and ^{123}I-MIBG for the simultaneous assessment of myocardial viability and sympathetic denervation. SPECT acquisition was performed in the supine position using a cardiac dedicated multi-pinhole cadmium–zinc–telluride (CZT) camera (Discovery NM 530c; General Electric Healthcare, Boston, Massachusetts, USA). Compton-corrected SPECT data were reconstructed as recently published [15]. Image analysis method has been published previously [15]. Patients underwent CMR imaging performed on a Siemens Magnetom Aera 1.5 T (Magnetom; Siemens, Erlangen, Germany). AAR assessment was obtained with a T2-weighted turbo echo spin inversion recovery and black blood protocol, without gadolinium injection (slice thickness 7 mm; repetition time 2 RR intervals; echo time 60 ms; image matrix 13×13). Scar size was obtained after a gadoteric acid injection (Dotarem; Guerbet, Villepinte, France) with a T1-weighted phase sensitive inversion recovery (Fig. 1). The images were analyzed using the OSIRIX post-processing software (OSIRIX; Pixmeo Sarl, Bernex, Switzerland) with manual contouring performed blinded to the SPECT analysis. SPECT and CMR imaging material and methods are detailed in Supplementary Appendices Section (Supplemental digital content 1, *http://links.lww.com/NMC/A120*). AAR was expressed as a percentage of total left ventricular myocardial area (%LV).

Statistical analysis

Categorical variables were expressed as frequencies and percentages; continuous variables were expressed as mean ± SD. Comparison between continuous variables was performed using appropriates *t*-tests (Wilcoxon test for paired nonparametric variables, Mann–Whitney test for unpaired nonparametric variables, and Student's *t*-test for parametric variables). Correlations between CMR and SPECT were calculated using a linear regression model. Correlation coefficients were compared using Spearman's ρ (R) coefficient. Statistical significance was accepted for two-sided P values less than 0.05. The statistical package GraphPad Prism 6.0 version (Graphpad Software Inc., La Jolla, California, USA) was used for statistical analysis.

Results

Patient population

A total of 36 patients were initially enrolled. One (2.7%) patient was excluded because of delayed revascularization 24 h after the onset of symptoms. 35 patients (27 men, eight women, age: 55.4 ± 10.2 years) were finally included for statistical analysis. Patients' baseline characteristics are summarized in Table 1. Most of them received the recommended medication. There was 62.9% of anterior wall STEMIs and most of patients had multivessel coronary artery disease (CAD) (57.1%).

SPECT study

The SPECT imaging protocol was acquired 13.3 ± 7.3 days after STEMI. The baseline results of SPECT study are shown in Table 2. ^{201}Tl SPECT showed a mean necrosis score of 15.4 ± 6.0 and necrosis area of 16.1 ± 14.4%LV. ^{123}I-MIBG SPECT, analyzing sympathetic myocardial denervation, showed a wider denervated area (51.1 ± 16.0% LV, $P < 0.0001$) in comparison with necrosis score and area (see illustration in Fig. 1). The mismatch of viable but denervated area was extended on 35.2 ± 14.2%LV.

Fig. 1

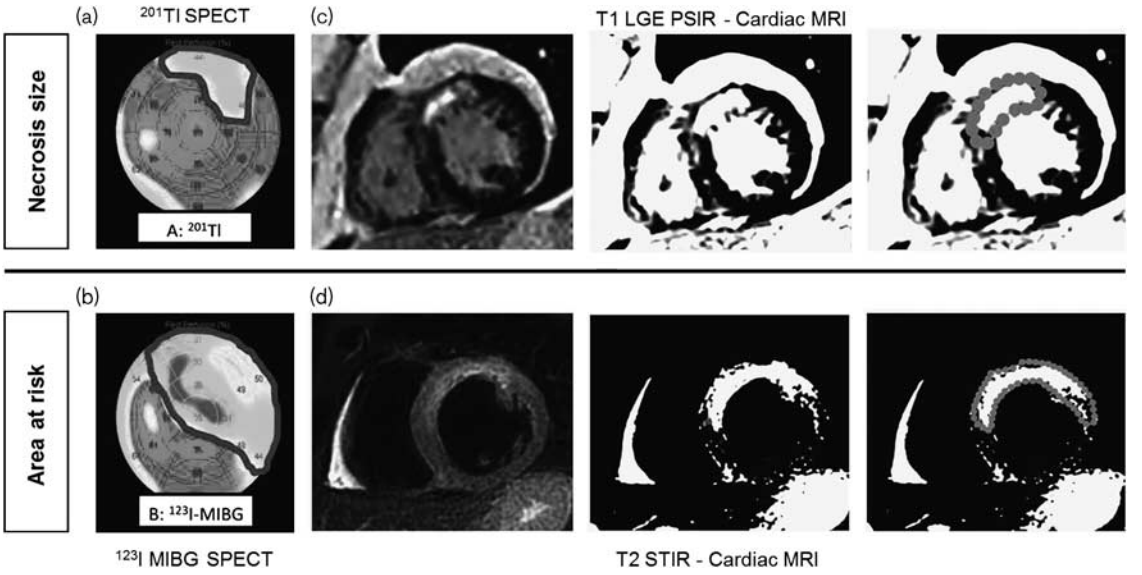

Illustration of cardiac magnetic resonance and single-photon emission computed tomography (SPECT) assessment after early revascularization of an acute anterior STEMI. Thallium-201 (^{201}Tl) imaging shows a limited necrosis myocardial area (a), iodine-123-meta-iodobenzylguanidine (^{123}I-MIBG) imaging shows a wide sympathetic denervated myocardial area reflecting the area at risk (b). Hyperintense short axis T2-weighted spin-echo turbo inversion recovery (STIR) (c) and late gadolinium enhancement (LGE) on T1-weighted phase-sensitive inversion recovery (PSIR) (d). For each MRI sequence: adjusted image window based on three regions of interest on normal myocardium (as described in the Patients and methods section) and manual contouring of the hyperintensive myocardium.

In subgroups analysis, we found no difference in necrosis area or denervated area in case of diabetes ($P=0.80$ and 0.48, respectively), dyslipidemia ($P=0.74$ and 0.26, respectively), or smoking habits ($P=0.70$ and 0.93, respectively). The denervated area was higher in case of hypertension (56.5 ± 11.5 vs. 47.2 ± 17.9%LV; $P=0.04$), but the necrosis area and myocardial mismatch were not different ($P=0.28$ and 0.14, respectively). According to the coronary status, we found no significant difference in denervated area size in case of three-vessel CAD patients ($P=0.26$). However, anterior wall STEMIs had wider denervated areas (56.7 ± 16.5 vs. 41.8 ± 10.0%LV; $P=0.0029$) and a trend for higher myocardial mismatch (38.3 ± 14.7 vs. 29.9 ± 12.1%LV; $P=0.09$), with similar necrosis size (18.6 ± 16.3 vs. 11.9 ± 9.4%LV; $P=0.29$) in comparison with the nonanterior wall STEMIs. The mismatch size was not influenced by the time to reperfusion ($P=0.36$). To confirm this information and trends on subgroups, we retrospectively analyzed 51 more SPECTs from other STEMI patients performed during the same period ($N=86$ patients). These 51 more patients did unfortunately undergo CMR acquisition. We found then that three-vessel CAD patients had a significantly lower mismatch area than patients with one-vessel or two-vessel CAD (19.9 ± 18.6 vs. 27.7 ± 16.0% LV; $P=0.03$). Anterior wall STEMIs had higher denervated areas (45.3 ± 21.7 vs. 34.7 ± 13.9%LV; $P=0.0052$) and higher myocardial mismatch (32.5 ± 18.4 vs. 18.6 ± 12.6%LV; $P=0.0002$), but with similar necrosis size (16.2 ± 17.3 vs. 19.6 ± 16.0%LV; $P=0.19$) than the nonanterior wall STEMIs.

Correlation between SPECT and CMR assessment

CMR was performed in the same delay than SPECT acquisition (12.1 ± 9.0 vs. 13.3 ± 7.3 days; $P=0.23$). Baseline results of SPECT and CMR studies are shown in Table 3. AAR assessed by CMR was 48.2 ± 12.0%LV and transmural necrosis extension was 18.7 ± 13.3%LV. Myocardial salvage was 30.0 ± 10.9%LV. In terms of the transmural necrosis size, the correlation between ^{201}Tl SPECT and transmural necrosis size on CMR assessment was good [Spearman's test ρ $(R)=0.86$, $P<0.0001$; Fig. 2a]. However, transmural and nontransmural necrosis, taken together, were significantly more observed in CMR than ^{201}Tl SPECT ($P<0.0001$). There was no difference between denervation on ^{123}I-MIBG SPECT and AAR assessment by CMR ($P=0.23$) and there was a moderate correlation [Spearman's correlation test $(R)=0.56$, $P=0.0002$; Fig. 2b]. Myocardial salvage evaluated by dual ^{201}Tl and ^{123}I-MIBG SPECT imaging was significantly higher than CMR assessment ($P=0.02$), and the correlation between the two techniques was nonsignificant (Fig. 2c). The difference in salvage evaluation between CMR and dual ^{201}Tl and ^{123}I-MIBG SPECT was not influenced by patient age ($P=0.9$), BMI ($P=0.54$), time to reperfusion ($P=0.69$), the higher troponin rate ($P=0.36$) or higher CRP rate ($P=0.85$), and time between SPECT and CMR assessment ($P=0.62$) or post-STEMI LVEF ($P=0.22$).

Table 1 Baseline characteristics of the study population ($n = 35$)

	Values
Sex	
Men	27 (77.1)
Women	8 (22.9)
Age (years)	55.4 ± 10.2
BMI (kg/m^2)	27.4 ± 3.6
Cardiovascular risk factors	
Diabetes	6 (17.1)
Hypertension	15 (42.9)
Hypercholesterolemia	9 (25.7)
Smoking	22 (62.9)
Family history of CAD	4 (11.4)
LVEF (%)	47.4 ± 10.4
Single-vessel CAD	15 (42.9)
Multivessel CAD	20 (57.1)
STEMI territory	
Anterior wall STEMI	22 (62.9)
Lateral or inferolateral wall STEMI	9 (25.7)
Inferior wall STEMI	4 (11.4)
Occluded artery	
Left anterior descending or diagonal	22 (62.9)
Left circumflex or marginal	5 (14.3)
Right coronary	8 (22.9)
Time to reperfusion (h)	3.2 ± 2.0
Biology	
CRP peak	50.0 ± 54.7
Troponin admission (hs-cTnT) (ng/l)	3612.0 ± 5426.0
Troponin peak (hs-cTnT) (ng/l)	7358.0 ± 4611.0
Medication use at discharge	
Platelet aggregation inhibitor	35 (100)
Statin	34 (97.1)
β-Blocker	35 (100)
Amiodarone	2 (5.7)
ACE inhibitor	33 (94.3)
Time STEMI to exam (days)	
Time to SPECT	12.8 ± 8.2
Time to CMR	12.1 ± 9.0
P	0.61

Values are expressed as *n* (%) and mean ± SD.
ACE, angiotensin-converting enzyme; CAD, coronary artery disease; CMR, cardiac magnetic resonance; CRP, C-reactive protein; hs-cTnT, high-sensitivity cardiac troponin T; LVEF, left ventricular ejection fraction; SPECT, single-photon emission computed tomography; STEMI, ST-elevation myocardial infarction.

Table 2 Baseline variables of ^{201}Tl and ^{123}I-MIBG SPECT imaging ($n = 35$)

	Values
Myocardial perfusion imaging (^{201}Tl)	
Necrosis score	15.4 ± 6.0
Necrosed area (%LV)	16.1 ± 14.4
Sympathetic myocardial denervation imaging (^{123}I-MIBG)	
Late H/M ratio	1.6 ± 0.14
Cardiac washout rate (%)	25.1 ± 10.5
Denervated score	23.8 ± 5.9
Denervated area (%LV)	51.1 ± 16.0
Denervation/necrosis mismatch	
Mismatch score	11.6 ± 7.2
Mismatch area (%LV)	35.2 ± 14.2

Values are expressed as mean ± SD.
H/M, heart/mediastin; ^{123}I-MIBG, iodine-123-meta-iodobenzylguanidine; %LV, percentage of left ventricular area; SPECT, single-photon emission computed tomography; ^{201}Tl, thallium-201.

Discussion

Our main results suggest that cardiac sympathetic denervation evaluated by ^{123}I-MIBG SPECT after STEMI could be a good tool for AAR estimation, with a good correlation compared with the current gold-standard CMR. Importantly, the ^{123}I-MIBG SPECT can be performed even late after the STEMI, paving the way for the use of this technique in clinical research.

Scar size quantification

As shown previously, myocardial necrosis assessment by ^{201}Tl SPECT defect was correlated strongly with transmural necrosis on CMR [4]. However, CMR systematically detects subendocardial infarcts that are missed by ^{201}Tl SPECT [16]. This difference is particularly important in case of small necrosis because of the higher sensitivity of CMR in comparison with ^{201}Tl SPECT [17].

AAR quantification

MIBG is indeed an analog of norepinephrine [18] and shares similar molecular mechanisms (uptake, storage). Low ^{123}I-MIBG fixation is then correlated with low sympathetic nerve activity in the myocardium. In HF, cardiac sympathetic denervation has already been adequately evaluated as a factor of worse outcome [11]. We choose a population of patients naive from HF to warranty that 123-MIBG disturbance were only due to the post STEMI denervation disturbances [19]. However, the impact of cardiac denervation after STEMI is still not accurately established.

Here, cardiac denervation assessed by ^{123}I-MIBG SPECT was more extensive than necrosis and its extent was independent compared with the time to reperfusion, suggesting that cardiac denervation might only be because of the initial ischemia, confirming the role of early reperfusion, saving as much myocardium as possible from necrosis (thus increasing the myocardial salvage area). Similar results were found in previous studies and could be explained by a higher sensitivity in neuronal cells hypoxia in comparison with myocardial cells [13]. Matsunari *et al.* [13] compared the AAR assessment by technetium-99m (^{99m}Tc)-sestamibi SPECT and ^{123}I-MIBG SPECT. AAR was more extensive than necrosis and both ^{99m}Tc-sestamibi before reperfusion and ^{123}I-MIBG SPECT yielded the same extent of AAR with high correlation ($R = 0.905$, $P < 0.001$). In a population of ischemic HF patients, Kasama *et al.* [20] and Simoes *et al.* [21] found that the denervation extension (assessed by ^{123}I-MIBG SPECT) was correlated with worst outcomes. The same conclusion was observed in case of both regional impairment of sympathetic tone and postmyocardial edema in a smaller population ($n = 10$) [14]. SPECT modalities could then provide prognostic information in addition to infarct size and LVEF reduction, emphasizing specific follow-up of this population.

The resulting myocardial salvage

The difference in myocardial salvage in our study may be explained, at least partly, by the underestimation of scar tissue size with ^{201}Tl SPECT in comparison with CMR

Table 3 SPECT and CMR comparison of myocardial areas after STEMI ($n = 35$ patients)

	SPECT				
	^{201}Tl	^{123}I-MIBG	CMR	*P*	Spearman's ρ (*P*)
Necrosis (%LV)	16.1 ± 14.4	–	Transmural necrosis: 18.7 ± 13.3	0.10	**0.86** (**0.0001**)
			Whole necrosis (nontransmural necrosis): 28.2 ± 14.5	**< 0.0001**	NS
Area at risk (%LV)	–	51.1 ± 16.0	48.2 ± 12.0	0.23	**0.56** (**0.0002**)
Salvage (%LV)	35.2 ± 14.2		30.0 ± 10.9	**0.02**	NS

Values are expressed as mean ± SD.
CMR, cardiac magnetic resonance; ^{123}I-MIBG, iodine-123-meta-iodobenzylguanidine; %LV, percentage of left ventricular area; SPECT, single-photon emission computed tomography; STEMI, ST-elevation myocardial infarction; ^{201}Tl, thallium-201.
The correlation index is Spearman's ρ (*R*).
Bold values statistically significant ($P < 0.05$).

because of subendocardial infarcts in our population. However, both methods are known to underestimate the viability compared with myocardial PET. CMR could provide a less underestimated evaluation, which could have led to such a difference. Finally, the underestimated AAR by CMR could also explain these results. Hadamitzky *et al.* [4] also found significantly smaller salvage area in CMR compared with SPECT (difference -2.8 ± 11.5, $P = 0.0015$) using a different SPECT technique of ^{99m}Tc-sestamibi administration before reperfusion. A direct comparison between various imaging approaches in animal models could provide additional data to better understand these discrepancies and respective interests.

Limitations of AAR assessment by CMR and comparison with SPECT

Comparison between CMR and ^{123}I-MIBG SPECT for the AAR seems possible, even though they are based on different physical basis and pathophysiologic pathways. CMR, measuring myocardial edema, has been proposed in many animals or human studies for AAR determination [22], but is largely debated [23]. Indeed, myocardial edema estimated by CMR follows a bimodal pattern: initial (within the 24 first hours) and deferred waves [24]. The deferred wave of edema appears progressively and is maximal around day 7 after reperfusion.

The validity of T2-weighted CMR for the assessment of the AAR has been called into question from the very beginning of its use for imaging myocardial edema. Recently, Kim *et al.* [25] has provided new evidence that T2-weighted CMR might not well delineate the ischemic AAR.

^{123}I-MIBG SPECT imaging is based on molecular mechanisms and thus on the pathophysiological fact that cardiac denervation of sympathetic nerves is because of initial ischemia [12] and the fact that neuronal cells are more sensitive to ischemia than myocardial cells [13]. This technique thus appears to be a promising alternative for AAR estimation.

However, it remains important to confirm whether this technique could become widely available, easy to perform, and analyze, eventually less expensive in comparison with CMR. It is important to keep in mind the radiation exposure of the SPECT technic [92 MBq of ^{201}Tl (15.7 mSv) and 185 MBq of ^{123}I-MIBG (2.6 mSv) led to a mean cumulated whole-body effective dose of 18.3 mSv in our population] and the possible limitations in specific populations (e.g. obese patients). Importantly, MIBG does not contribute much toward the whole irradiation.

Study limitations and perspectives

The number of patients is small (only 35 patients). SPECT and CMR imaging should be compared in more patients to corroborate the reliability and consistency of our results. Second, we do not know the evolution of denervation over time. It has been shown that the post-STEMI treatments may modify myocardial denervation, and thus denervation assessment, increasing sympathetic nerve activity. However, the impact of medication for a maximum of 10 days after STEMI should be negligible [26].

To our knowledge, our study is the first to compare prospectively ^{123}I-MIBG SPECT and CMR assessments of AAR with a rigorous method of area size quantification. PET imaging has superior quantitative capabilities. However, ^{123}I-MIBG SPECT is nowadays the only widely available imaging technic for the sympathetic innervation assessment [27]. It is well established that ^{123}I-MIBG SPECT can contribute toward risk stratification for lethal events [12]. In addition, this imaging might help select patients who are more suitable for implantable cardioverter defibrillator (ICD) implantation or cardiac resynchronization therapy, particularly when associated with HF. This strategy could reduce the rate of complication because of noneffective ICD implantation, in addition to a cost reduction benefit. A specific study might be useful to evaluate the ability to assist physicians in selecting patients for ICD implantation. As cardioprotective pharmacological strategies have already been proven to improve cardiac innervation after myocardial infarction, a strategy guided by ^{123}I-MIBG SPECT could enable titration and efficiency monitoring [28].

Fig. 2

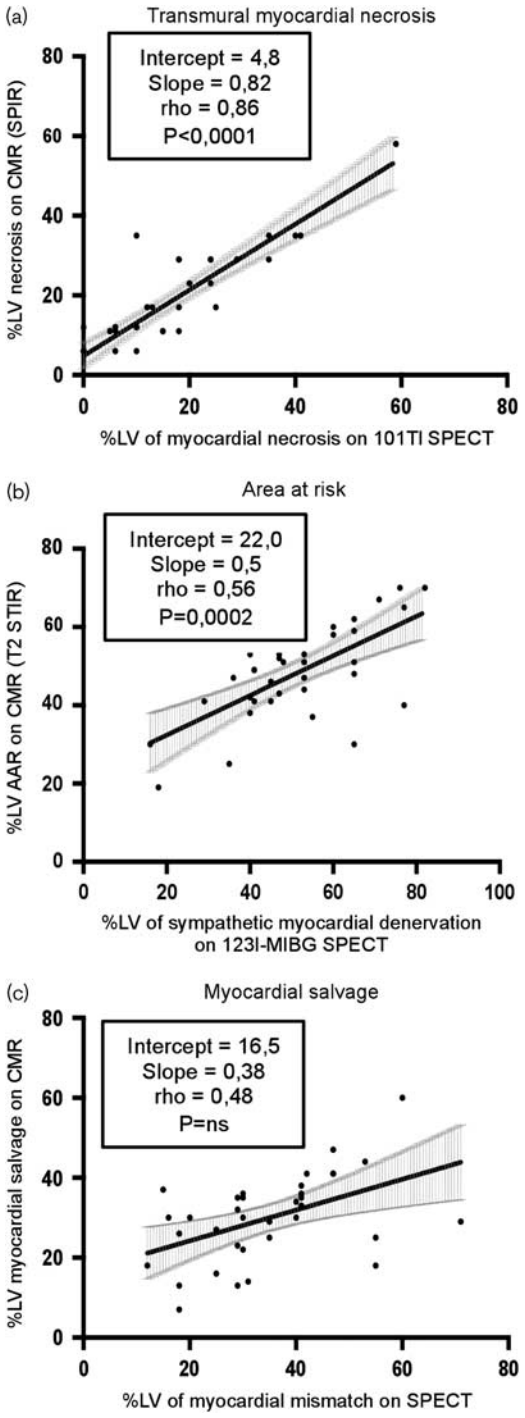

Correlation between single-photon emission computed tomography (SPECT) and cardiac magnetic resonance (CMR), $n = 35$ patients. Nonparametric *t*-tests and Spearman's correlation ρ (R) between CMR and SPECT for myocardial necrosis (a), area at risk (AAR) (b), and myocardial salvage (c). Hatched areas represent the 95% confidence interval of the correlation index. Some points coincide with the origin of axis in case of absence of necrosis. ^{123}I-MIBG, iodine-123-meta-iodobenzylguanidine; %LV, percentage of left ventricular area.

Conclusion

Our study shows that the postmyocardial sympathetic denervation after a STEMI can be evaluated by ^{123}I-MIBG SPECT and is correlated with the AAR assessed by CMR. CMR and SPECT, even if adequately correlated, are based on different imaging evaluations and reflect distinct pathophysiologic pathways. These two techniques could then be considered as two sides of the same coin, providing additional information.

Acknowledgements

C.H. and F.H. performed patient recruitment, data collection, and statistical analysis; F.L., F.C., S.C., R.G., J.C.M. performed patient recruitment; H.V., D.M.G., M.B., F.B.B., F.V., M.D., and A.B. carried out image analysis of SPECT or MRI; D.V. provided language help and writing assistance; F.R., D.M.G. provided the initial idea, team management and patient recruitment.

Conflicts of interest

There are no conflicts of interest.

References

1 Reimer KA, Jennings RB. The 'wavefront phenomenon' of myocardial ischemic cell death. II. Transmural progression of necrosis within the framework of ischemic bed size (myocardium at risk) and collateral flow. *Lab Invest* 1979; **40**:633–644.

2 Authors/Task Force Members, Windecker S, Kolh P, Alfonso F, Collet JP, Cremer J, *et al.* 2014 ESC/EACTS Guidelines on myocardial revascularization: The Task Force on Myocardial Revascularization of the European Society of Cardiology (ESC) and the European Association for Cardio-Thoracic Surgery (EACTS). Developed with the special contribution of the European Association of Percutaneous Cardiovascular Interventions (EAPCI). *Eur Heart J* 2014; **35**:2541–2619.

3 McAlindon E, Pufulete M, Lawton C, Angelini GD, Bucciarelli-Ducci C. Quantification of infarct size and myocardium at risk: evaluation of different techniques and its implications. *Eur Heart J Cardiovasc Imaging* 2015; **16**:738–746.

4 Hadamitzky M, Langhans B, Hausleiter J, Sonne C, Kastrati A, Martinoff S, *et al.* The assessment of area at risk and myocardial salvage after coronary revascularization in acute myocardial infarction: comparison between CMR and SPECT. *JACC Cardiovasc Imaging* 2013; **6**:358–369.

5 Matsumoto H, Matsuda T, Miyamoto K, Shimada T, Mikuri M, Hiraoka Y. Peri-infarct zone on early contrast-enhanced cmr imaging in patients with acute myocardial infarction. *JACC Cardiovasc Imaging* 2011; **4**:610–618.

6 Barber MJ, Mueller TM, Henry DP, Felten SY, Zipes DP. Transmural myocardial infarction in the dog produces sympathectomy in noninfarcted myocardium. *Circulation* 1983; **67**:787–796.

7 Dae MW, Herre JM, O'Connell JW, Botvinick EH, Newman D, Munoz L. Scintigraphic assessment of sympathetic innervation after transmural versus nontransmural myocardial infarction. *J Am Coll Cardiol* 1991; **17**:1416–1423.

8 Van der Veen BJ, Al Younis I, de Roos A, Stokkel MP. Assessment of global cardiac I-123 MIBG uptake and washout using volumetric quantification of SPECT acquisitions. *J Nucl Cardiol* 2012; **19**:752–762.

9 Hendel RC, Berman DS, Carli MFD, Heidenreich PA, Henkin RE, Pellikka PA, *et al.* ACCF/ASNC/ACR/AHA/ASE/SCCT/SCMR/SNM 2009 Appropriate Use Criteria for Cardiac Radionuclide Imaging A Report of the American College of Cardiology Foundation Appropriate Use Criteria Task Force, the American Society of Nuclear Cardiology, the American College of Radiology, the American Heart Association, the American Society of Echocardiography, the Society of Cardiovascular Computed Tomography, the Society for Cardiovascular Magnetic Resonance, and the Society of Nuclear Medicine: Endorsed by the American College of Emergency Physicians. *Circulation* 2009; **119**:e561–e587.

10 Shen YT, Knight DR, Thomas JX, Vatner SF. Effects of selective cardiac denervation on collateral blood flow after coronary artery occlusion in conscious dogs. *Basic Res Cardiol* 1990; **85** (**Suppl 1**):229–239.
11 Jacobson AF, Senior R, Cerqueira MD, Wong ND, Thomas GS, Lopez VA, *et al*. Myocardial iodine-123 meta-iodobenzylguanidine imaging and cardiac events in heart failure. Results of the prospective ADMIRE-HF (AdreView Myocardial Imaging for Risk Evaluation in Heart Failure) study. *J Am Coll Cardiol* 2010; **55**:2212–2221.
12 Boogers MJ, Borleffs CJW, Henneman MM, van Bommel RJ, van Ramshorst J, Boersma E, *et al*. Cardiac sympathetic denervation assessed with 123-iodine metaiodobenzylguanidine imaging predicts ventricular arrhythmias in implantable cardioverter-defibrillator patients. *J Am Coll Cardiol* 2010; **55**:2769–2777.
13 Matsunari I, Schricke U, Bengel FM, Haase HU, Barthel P, Schmidt G, *et al*. Extent of cardiac sympathetic neuronal damage is determined by the area of ischemia in patients with acute coronary syndromes. *Circulation* 2000; **101**:2579–2585.
14 Gimelli A, Masci PG, Liga R, Grigoratos C, Pasanisi EM, Lombardi M, *et al*. Regional heterogeneity in cardiac sympathetic innervation in acute myocardial infarction: relationship with myocardial oedema on magnetic resonance. *Eur J Nucl Med Mol Imaging* 2014; **41**:1692–1694.
15 D'estanque E, Hedon C, Lattuca B, Bourdon A, Benkiran M, Verd A, *et al*. Optimization of a simultaneous dual-isotope (201)Tl/(123)I-MIBG myocardial SPECT imaging protocol with a CZT camera for trigger zone assessment after myocardial infarction for routine clinical settings: Are delayed acquisition and scatter correction necessary? *J Nucl Cardiol* 2017; **24**:1361–1369.
16 Wagner A, Mahrholdt H, Holly TA, Elliott MD, Regenfus M, Parker M, *et al*. Contrast-enhanced MRI and routine single photon emission computed tomography (SPECT) perfusion imaging for detection of subendocardial myocardial infarcts: an imaging study. *Lancet* 2003; **361**:374–379.
17 Ibrahim T, Nekolla SG, Hörnke M, Bülow HP, Dirschinger J, Schömig A, *et al*. Quantitative measurement of infarct size by contrast-enhanced magnetic resonance imaging early after acute myocardial infarction: comparison with single-photon emission tomography using Tc99m-sestamibi. *J Am Coll Cardiol* 2005; **45**:544–552.
18 Wieland DM, Wu J, Brown LE, Mangner TJ, Swanson DP, Beierwaltes WH. Radiolabeled adrenergi neuron-blocking agents: adrenomedullary imaging with [^{131}I]iodobenzylguanidine. *J Nucl Med* 1980; **21**:349–353.
19 Marini C, Giorgetti A, Gimelli A, Kusch A, Sereni N, L'abbate A, *et al*. Extension of myocardial necrosis differently affects MIBG retention in heart failure caused by ischaemic heart disease or by dilated cardiomyopathy. *Eur J Nucl Med Mol Imaging* 2005; **32**:682–688.
20 Kasama S, Toyama T, Sumino H, Kumakura H, Takayama Y, Minami K, *et al*. Prognostic value of cardiac sympathetic nerve activity evaluated by [^{123}I] m-iodobenzylguanidine imaging in patients with ST-segment elevation myocardial infarction. *Heart* 2011; **97**:20–26.
21 Simões MV, Barthel P, Matsunari I, Nekolla SG, Schömig A, Schwaiger M, *et al*. Presence of sympathetically denervated but viable myocardium and its electrophysiologic correlates after early revascularised, acute myocardial infarction. *Eur Heart J* 2004; **25**:551–557.
22 Friedrich MG, Abdel-Aty H, Taylor A, Schulz-Menger J, Messroghli D, Dietz R. The salvaged area at risk in reperfused acute myocardial infarction as visualized by cardiovascular magnetic resonance. *J Am Coll Cardiol* 2008; **51**:1581–1587.
23 Kim RJ, Fieno DS, Parrish TB, Harris K, Chen EL, Simonetti O, *et al*. Relationship of MRI delayed contrast enhancement to irreversible injury, infarct age, and contractile function. *Circulation* 1999; **100**:1992–2002.
24 Fernández-Jiménez R, Fuster V, Ibáñez B. Reply: myocardial edema should be stratified according to the state of cardiomyocytes within the ischemic region. *J Am Coll Cardiol* 2015; **65**:2356–2357.
25 Kim HW, van Assche L, Jennings RB, Wince WB, Jensen CJ, Rehwald WG, *et al*. Relationship of T2-weighted MRI myocardial hyperintensity and the ischemic area-at-risk. *Circ Res* 2015; **117**:254–265.
26 Ciarka A, van de Borne P, Pathak A. Myocardial infarction, heart failure and sympathetic nervous system activity: new pharmacological approaches that affect neurohumoral activation. *Expert Opin Investig Drugs* 2008; **17**:1315–1330.
27 Dimitriu-Leen AC, Scholte AJHA, Jacobson AF. ^{123}I-MIBG SPECT for evaluation of patients with heart failure. *J Nucl Med* 2015; **56**:25s–30s.
28 Nakata T, Nakata K, Hashimoto A. Recent developments and future directions of sympathetic nervous function imaging. *Ann Nucl Cardiol* 2016; **2**:146–151.